


Axion–Sterile Neutrino Dark Matter

Alberto Salvio ^{1,2,*} and Simone Scollo ¹ 

¹ Physics Department, University of Rome Tor Vergata, Via Della Ricerca Scientifica, I-00133 Rome, Italy; simone.scollo1@gmail.com

² I. N. F. N.—Rome Tor Vergata, Via Della Ricerca Scientifica, I-00133 Rome, Italy

* Correspondence: alberto.salvio@roma2.infn.it

Abstract: Extending the standard model with three right-handed neutrinos and a simple QCD axion sector can account for neutrino oscillations, dark matter and baryon asymmetry; at the same time, it solves the strong CP problem, stabilizes the electroweak vacuum and can implement critical Higgs inflation (satisfying all current observational bounds). We perform here a general analysis of dark matter (DM) in such a model, which we call the ν MSM. Although critical Higgs inflation features a (quasi) inflection point of the inflaton potential, we show that DM cannot receive a contribution from primordial black holes in the ν MSM. This leads to a multicomponent axion–sterile neutrino DM and allows us to relate the axion parameters, such as the axion decay constant, to the neutrino parameters. We include several DM production mechanisms: the axion production via misalignment and decay of topological defects as well as the sterile neutrino production through the resonant and non-resonant mechanisms and in the recently proposed CPT-symmetric universe.

Keywords: neutrinos; axion; inflation



check for updates

Citation: Salvio, A.; Scollo, S. Axion–Sterile Neutrino Dark Matter. *Universe* **2021**, *7*, 354. <https://doi.org/10.3390/universe7100354>

Academic Editor: Norma G. Sanchez

Received: 26 August 2021

Accepted: 16 September 2021

Published: 23 September 2021

Publisher's Note: MDPI stays neutral with regard to jurisdictional claims in published maps and institutional affiliations.



Copyright: © 2021 by the authors. Licensee MDPI, Basel, Switzerland. This article is an open access article distributed under the terms and conditions of the Creative Commons Attribution (CC BY) license (<https://creativecommons.org/licenses/by/4.0/>).

1. Introduction

Despite the remarkable success of the standard model (SM), there is no question that it needs to be extended. The observational evidence for neutrino oscillations and DM is indeed enough to draw this conclusion.

A minimal phenomenological completion of the SM up to the Planck scale was presented in [1], where the SM was extended to include three right-handed neutrinos with a generic flavor structure and the extra fields of the simplest invisible QCD axion model, the KSVZ one [2,3]. The model of [1], which we refer to as the ν MSM, not only accounts for neutrino oscillations and DM, but it can also provide the observed amount of baryon asymmetry in the universe, stabilize the electroweak (EW) vacuum, realize Higgs inflation [4–7] and solve the strong CP problem through the Peccei–Quinn (PQ) symmetry¹ [11,12] at the same time.

In Ref. [13], it was found that Higgs inflation can be realized in its critical version [14–16] within the ν MSM: critical Higgs inflation (CHI) occurs when the SM lies extremely close to the border between the absolute stability and metastability of the EW vacuum [17]. CHI is particularly interesting for two reasons. One is that it can occur with a moderate, $\mathcal{O}(10)$, non-minimal coupling ξ_H between the Higgs and the Ricci scalar. Consequently, the scale of breaking of perturbative unitarity, which was noticed in [18–22], is pushed just below the Planck scale where new physics is required to UV complete gravity. Furthermore, in Ref. [23], it was shown that CHI, unlike standard Higgs inflation [24], does not suffer from fine tuning in the initial conditions before inflation. It is also interesting that one will be able to test this inflationary scenario with future space-borne interferometers [25].

To date, DM in this model has been accounted for exclusively through the axion. However, the ν MSM is rich enough to contain other potential DM candidates. DM is one of the biggest mysteries in fundamental physics, it represents the majority of matter in our universe, but its nature is still unclear. Motivated by these and other facts (see below), here we perform a general analysis of DM in the ν MSM.

We now provide an outline of this paper, which includes a summary of the results and highlights the motivations and the original parts.

In Section 2, we briefly review the ν MSM. The gauge group, $SU(3)_c \times SU(2)_L \times U(1)_Y$, is the same as that of the SM, but the field content is extended to include the three right-handed neutrinos, a complex scalar (gauge singlets) and two Weyl fermions that are charged under the color gauge factor $SU(3)_c$ only. The gravitational sector includes non-minimal couplings of all scalars to gravity, which allow inflation to take place. Section 2 also includes a discussion of the generic observational bounds that are needed for our purposes (other than the bounds related to DM, which are then discussed in the following sections).

Section 3 focuses on the axion contribution to DM. As explained there, we include the contribution from both the misalignment mechanism [26–28] and the decay of topological defects [29–36], which have been computed for the KSVZ model in [37]. The latter contribution to the DM energy density has a dependence on the quartic coupling of the extra scalar, whose value in the relevant parameter space of the ν MSM is determined here explicitly.

Sections 4 and 5 are dedicated to the contribution to DM due to the lightest sterile neutrino. This is a good warm dark matter candidate when its mass is around the keV. Three possible mechanisms are found. The first two are the non-resonant [38] and resonant [39] production mechanisms, which occur thanks to the mixing between this sterile neutrino and the active neutrinos of the SM (see Refs. [40–42] for reviews). The third one takes place in a recently proposed CPT-symmetric universe [43,44], where inflation and the above-mentioned mixing are not required. For all these mechanisms, we derive the contributions to the DM energy density and the observational bounds as functions of the DM fraction X_s due to the lightest sterile neutrino. Some of these functions were already known in the literature, while others are extracted here, as discussed in those sections.

Since in all the sterile neutrino production mechanisms the masses of these neutral fermions are below the $\sim 10^{14}$ GeV scale, they necessarily have a negligible impact on the running and, consequently, the parameter space of the ν MSM with absolute EW vacuum stability is enlarged [1]. This is because, generically, a Yukawa coupling (that is proportional to the mass of a fermion) contributes negatively to the β -function of the Higgs quartic coupling, as explained at the end of Section 5. Furthermore, the presence of a sizeable sterile neutrino contribution to DM, as we will discuss explicitly, allows the reduction of the mass of the extra scalar for fixed values of its couplings and so stabilization of the EW vacuum more efficiently [1,13,45,46]. All the sterile neutrino production mechanisms, therefore, favor EW vacuum stability. This is another motivation for realizing a fraction of DM through sterile neutrinos in the ν MSM.

Yet another motivation for this work is the fact that the well-motivated presence of the axion also significantly enlarges the viable region of parameter space for sterile neutrino DM in the ν MSM, compared to the case² $X_s = 1$ (where this region is quite narrow [52,53]): all observational bounds become weaker when the sterile neutrino has to account for only a fraction $X_s < 1$ of DM.

Another possible source of DM in the ν MSM could be due to primordial black holes (PBHs): CHI features a (quasi) inflection point in the inflaton potential, which has been proposed in [54–58] as a potential trigger for PBH DM production (see Ref. [59] for a review). However, in Section 6, we show that, although this feature is qualitatively present, the ν MSM is not quantitatively able to account for any fraction of DM in the form of PBHs.

Therefore, the ν MSM leads to an axion–sterile neutrino DM scenario, which allows us to relate the axion parameters such as the axion decay constant f_a to the sterile neutrino parameters (the masses of these neutral particles and their mixing with the active neutrinos); this provides us with an interesting link between neutrino and axion physics. The allowed parameter space for this combined axion–sterile neutrino DM scenario is identified in Section 7 taking into account the previously discussed bounds.

Finally, in Section 8 we offer our conclusions.

2. The ν MSM and Generic Observational Bounds

We now give the details of the ν MSM that are needed for our purposes (see Refs. [1,13] for an introduction to this model). The SM is extended with three sterile neutrinos N_i and the fields of the KSVZ axion model [2,3] (two Weyl fermions q_1, q_2 neutral under $SU(2)_L \times U(1)_Y$ and a complex scalar A).

Correspondingly, the SM Lagrangian, \mathcal{L}_{SM} , is extended by adding three terms,

$$\mathcal{L} = \mathcal{L}_{SM} + \mathcal{L}_N + \mathcal{L}_{\text{axion}} + \mathcal{L}_{\text{gravity}}, \tag{1}$$

which we define in turn. \mathcal{L}_N represents the N -dependent piece:

$$i\bar{N}_i \not{\partial} N_i + \left(\frac{1}{2} N_i M_{ij} N_j + Y_{ij} L_i H N_j + \text{h.c.} \right). \tag{2}$$

We take the Majorana mass matrix M diagonal and real, $M = \text{diag}(M_1, M_2, M_3)$, without loss of generality, but the Yukawa matrix Y is generic. $\mathcal{L}_{\text{axion}}$ is the KSVZ piece:

$$\mathcal{L}_{\text{axion}} = i \sum_{j=1}^2 \bar{q}_j \not{D} q_j + |\partial A|^2 - (y q_2 A q_1 + \text{h.c.}) - \Delta V(H, A),$$

where $\Delta V(H, A)$ is the A -dependent piece of the classical potential

$$\Delta V(H, A) \equiv \lambda_A (|A|^2 - f_a^2/2)^2 + \lambda_{HA} (|H|^2 - v^2) (|A|^2 - f_a^2/2),$$

$v \simeq 174$ GeV is the EW breaking scale and f_a is the axion decay constant. The Yukawa coupling y is chosen real and positive without loss of generality. Finally,

$$\mathcal{L}_{\text{gravity}} = - \left(\frac{\bar{M}_{\text{Pl}}^2}{2} + \zeta_H (|H|^2 - v^2) + \zeta_A (|A|^2 - f_a^2/2) \right) R - \Lambda, \tag{3}$$

where \bar{M}_{Pl} is the reduced Planck mass, R is the Ricci scalar, ζ_H and ζ_A are the non-minimal couplings of H and A to gravity and Λ is the cosmological constant. In our model, the inflaton is identified with the Higgs; it is possible to do so with $\zeta_H \sim \mathcal{O}(10)$, as discussed in Ref. [13], when we are close to the frontier between the stability and the metastability of the EW vacuum (critical Higgs inflation).

After EW symmetry breaking, the neutrinos acquire a Dirac mass matrix $m_D = vY$, which can be parameterized in terms of column vectors m_{Di} ($i = 1, 2, 3$), i.e., $m_D = (m_{D1}, m_{D2}, m_{D3})$. The active neutrino masses m_i ($i = 1, 2, 3$) are obtained by diagonalizing the matrix

$$m_\nu = \frac{m_{D1} m_{D1}^T}{M_1} + \frac{m_{D2} m_{D2}^T}{M_2} + \frac{m_{D3} m_{D3}^T}{M_3}. \tag{4}$$

We then express Y in terms of the M_i and m_i as done in Refs. [1,13].

On the other hand, the PQ symmetry breaking induced by $\langle A \rangle = f_a/\sqrt{2}$ leads to the quark mass $M_q = y f_a/\sqrt{2}$ and the scalar squared mass

$$M_A^2 = f_a^2 \left(2\lambda_A + \mathcal{O} \left(\frac{v^2}{f_a^2} \right) \right). \tag{5}$$

Since $f_a \gtrsim 10^8$ GeV (see Ref. [60] for a review), the $\mathcal{O}(v^2/f_a^2)$ term is very small and will be neglected.

Let us now discuss the other generic observational bounds that are relevant for our purposes³ (with the exception of the bounds related to DM, which will be discussed in the following sections). As far as the active neutrinos are concerned, we have several data from oscillation and non-oscillation experiments. For example, Refs. [61,62] presented

some of the most recent determinations of Δm_{21}^2 and Δm_{3l}^2 (where $\Delta m_{ij}^2 \equiv m_i^2 - m_j^2$ and $\Delta m_{3l}^2 \equiv \Delta m_{31}^2$ for normal ordering and $\Delta m_{3l}^2 \equiv -\Delta m_{32}^2$ for inverted ordering), as well as of the active neutrino mixing angles and the CP phase in the Pontecorvo–Maki–Nakagawa–Sakata (PMNS) matrix. Here, we take the currently most precise values reported in [61,62] for normal ordering (which is currently preferred). Regarding the SM sector, we also have to fix the values of the relevant SM couplings at the EW scale, say, at the top mass $M_t \simeq 172.5$ GeV [63]. We take the values computed in [17], which expresses these quantities in terms of M_t , the Higgs mass $M_h \simeq 125.1$ GeV [64], the strong fine-structure constant renormalized at the Z mass, $\alpha_s(M_Z) \simeq 0.1184$ [65] and $M_W \simeq 80.379$ GeV [64] (see the quoted literature for the uncertainties on these quantities).

3. Axion Dark Matter

As we will discuss, axion DM is produced in the av MSM by two mechanisms: the misalignment one [26–28] and the decay of topological defects [29–37]. In order to determine these contributions to DM, the topological susceptibility χ (given in terms of m_a by $\chi = m_a^2 f_a^2$) is needed. The axion mass m_a and thus χ are complicated functions of the temperature T . Here, we use the precise calculations of χ provided by [66,67].

As discussed in [37], the energy density ρ_a^{mis} due to axions produced by the misalignment mechanism contributes a fraction $\Omega_a^{\text{mis}} = \rho_a^{\text{mis}} / \rho_{\text{cr}}$ given by⁴

$$\Omega_a^{\text{mis}} h^2 = (0.12 \pm 0.02) \left(\frac{f_a}{1.92 \times 10^{11} \text{GeV}} \right)^{1.165}. \tag{6}$$

Requiring that the axion energy density does not exceed the total DM energy density ρ_{DM} (and using $\Omega_{\text{DM}} \equiv \rho_{\text{DM}} / \rho_{\text{cr}} = (0.1186 \pm 0.0020) / h^2$ [68]), we find the upper bound

$$f_a \lesssim 2 \times 10^{11} \text{ GeV} \quad (\text{from misalignment}). \tag{7}$$

Higgs inflation features a high reheating temperature, $T_{\text{RH}} \gtrsim 10^{13}$ GeV, thanks to the sizable couplings between the Higgs and other SM particles [69,70]. Thus, $T_{\text{RH}} \gg f_a$ and the PQ symmetry is restored after inflation in the av MSM.

Therefore, here, axion DM is also produced through decays of topological defects, which leads to a contribution $\rho_a^{\text{string}} \equiv \Omega_a^{\text{string}} \rho_{\text{cr}}$ to the energy density, which in our model is given by [37]

$$\Omega_a^{\text{string}} h^2 = 0.37_{-0.2}^{+0.3} \left(\frac{f_a}{1.92 \times 10^{11} \text{GeV}} \right)^{1.165} \frac{\ln(f_a t_{co} \sqrt{\lambda_A / \zeta})}{50}. \tag{8}$$

In Equation (8), the time t_{co} can be determined in terms of m_a by

$$\frac{2\pi\epsilon_a}{t_{co}} = m_a(t_{co}) \tag{9}$$

and the numerical simulations of [71] give $\epsilon_a = 4 \pm 0.7$ and $\zeta = 1 \pm 0.5$.

Therefore, the time t_{co} can be computed by using the precise calculations of χ . However, since Ω_a^{string} depends on t_{co} only logarithmically, we can, as we explain now, simply estimate t_{co} by using the dilute instanton gas approximation, which gives a power-law temperature dependence of χ ,

$$\chi(T) = \chi_0 \left(\frac{T_{\text{QCD}}}{T} \right)^n, \tag{10}$$

where T_{QCD} is the temperature of the QCD confining phase transition ($T_{\text{QCD}} \simeq 157$ MeV), $n \simeq 8.16$ and $\chi_0 \simeq 0.0216 \text{ fm}^{-4} \simeq (75.6 \text{ MeV})^4$ [67]. Here, our treatment starts to diverge from that of [37] because the quartic coupling λ_A does not need to be tiny in our model

(unlike in [37]). First, note that in the radiation dominated era the Friedmann equation can be written in the form

$$t^{-2} = \frac{2\pi^2}{45\bar{M}_{\text{Pl}}^2} g_*(T) T^4, \tag{11}$$

where g_* is the effective number of relativistic species. Using this result and Equations (9) and (10), one finds

$$T_{co} = \left(\frac{45\bar{M}_{\text{Pl}}^2 \chi_0 T_{\text{QCD}}^n}{8\pi^4 \epsilon_a^2 f_a^2 g_*} \right)^{\frac{1}{4+n}} \simeq \text{GeV} \left(\frac{2 \times 10^{11} \text{ GeV}}{f_a} \right)^{\frac{2}{4+n}} g_*^{-\frac{1}{4+n}}, \tag{12}$$

so

$$T_{co} \simeq 0.8 \text{ GeV} \left(\frac{2 \times 10^{11} \text{ GeV}}{f_a} \right)^{\frac{2}{4+n}}, \tag{13}$$

where we used well-known determinations of g_* in the SM (see, e.g., [67]) and the fact that the contributions of the extra particles beyond the SM to g_* are negligible at those temperatures. As a check of this result, note that the power-law temperature dependence of χ already fits reasonably well the full lattice results from temperatures of the order of a few hundred MeV (see Figure 2 of [67]). Now, using again the Friedmann equation in (11), we have

$$t_{co} \simeq 4 \times 10^{-7} \text{ s} \left(\frac{f_a}{2 \times 10^{11} \text{ GeV}} \right)^{\frac{4}{4+n}}. \tag{14}$$

We can equivalently use Equation (13) or Equation (14) to estimate the argument of the logarithm in (8) because (9) and (10) tell us

$$f_a t_{co} \sqrt{\lambda_A / \zeta} = \frac{2\pi \epsilon_a f_a^2 \sqrt{\lambda_A}}{\sqrt{\chi_0 \zeta}} \left(\frac{T_{co}}{T_{\text{QCD}}} \right)^{\frac{n}{2}}. \tag{15}$$

Therefore, Equation (13) or Equation (14) allows us to estimate Ω_a^{string} for each value of f_a and λ_A . So, fixing λ_A , we obtain a maximal value of f_a , which we call here f_a^{max} , from the requirement that the axion energy density does not exceed the total DM energy density ρ_{DM} , namely

$$\Omega_a^{\text{mis}} + \Omega_a^{\text{string}} \leq \Omega_{\text{DM}}, \tag{16}$$

where $\Omega_{\text{DM}} \equiv \rho_{\text{DM}} / \rho_{\text{cr}}$. If one considers, for example, $\lambda_A = 0.1$ the argument of the logarithm in (8) becomes

$$f_a t_{co} \sqrt{\lambda_A / \zeta} \simeq 4 \times 10^{28} \left(\frac{f_a}{2 \times 10^{11} \text{ GeV}} \right)^{\frac{8+n}{4+n}}. \tag{17}$$

and so

$$f_a \leq f_a^{\text{max}} \simeq 5 \times 10^{10} \text{ GeV} \quad (\text{for } \lambda_A = 0.1), \tag{18}$$

which is significantly lower than the pure misalignment bound in (7). In Figure 1, we show how f_a^{max} depends on λ_A .

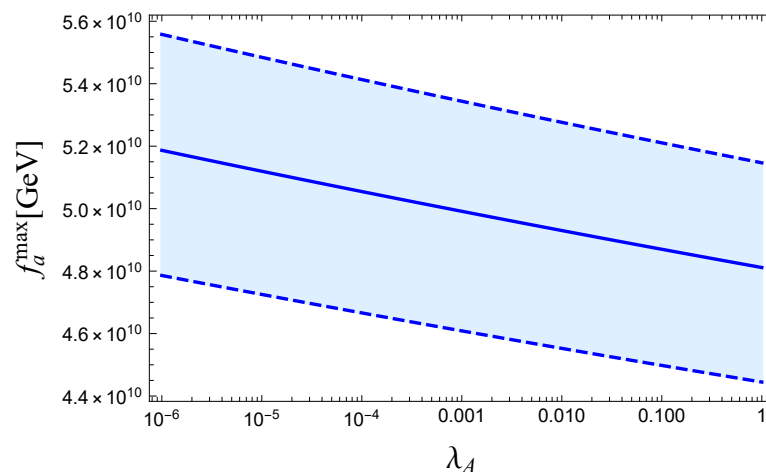


Figure 1. Dependence on λ_A of the maximal value of f_a obtained by requiring that DM is not overproduced in the ν MSM. The width of the band corresponds to the uncertainties in Equations (6) and (8).

4. Sterile Neutrino Dark Matter

Another important source of DM in the ν MSM is the sterile neutrino \tilde{N}_1 with the smallest mass m_s . Generically, this is not exactly N_1 due to an active–sterile neutrino mixing. Indeed, in an inflationary⁵ universe, the production of this particle occurs through its mixing with the active neutrinos of the SM. Such mixing is described by three (generically complex) quantities $\theta_{\alpha 1}$, where α represents the flavor of the active neutrino ν_α ($\alpha = e, \mu, \tau$). The $\theta_{\alpha 1}$ are the elements of the matrix $\Theta \equiv m_D M^{-1}$. It is convenient to introduce a total mixing parameter θ defined by [42]

$$\theta^2 \equiv \sum_{\alpha=e,\mu,\tau} |\theta_{\alpha 1}|^2. \tag{19}$$

The mixing with the active neutrinos leads to the production of sterile neutrinos in the early universe in two ways. One is provided by the oscillations between active and sterile states. Furthermore, sterile neutrinos are produced in scatterings. Though this production mechanism is “thermal” in the sense that the \tilde{N}_1 are produced in scatterings in a thermal plasma, generically these particles are not in thermal equilibrium because of their tiny couplings. As we will discuss in the following subsections, the energy density ρ_s of the lightest sterile neutrino can generically account for a non-negligible fraction X_s of the total DM abundance, i.e., $\Omega_s = X_s \Omega_{DM}$, where $\Omega_s = \rho_s / \rho_{cr}$ and $0 \leq X_s \leq 1$.

In order to identify the allowed regions of the parameter space, it is necessary to have the observational bounds for an arbitrary value of X_s . Of course, the bounds will be generically weaker for $X_s < 1$ than for $X_s = 1$, but we want to know how they change varying X_s .

First, a fermionic DM candidate is subject to a phase-space lower bound on its mass (also known as the Tremaine–Gunn bound [72]) that is related to Pauli’s exclusion principle⁶. The strongest information comes from the dwarf spheroidal galaxies (dSphs), which are the most compact DM-dominated objects observed to date. In objects of this sort, the dynamics of the DM particles can be characterized by some coarse-grained primordial phase-space density \mathcal{D} and the one-dimensional velocity σ ; see [74] for a detailed discussion. Since the coarse-grained phase-space density either remains constant or diminishes, today we have [74] (see also [75])

$$\frac{\rho_s}{\sigma^3} \leq 3^{3/2} m_s^4 \mathcal{D}. \tag{20}$$

Therefore, writing $\rho_s = X_s \rho_{DM}$, we obtain the lower mass bound

$$m_s \geq \left(\frac{X_s \rho_{DM}}{3^{3/2} \mathcal{D} \sigma^3} \right)^{1/4}. \tag{21}$$

This result tells us that the phase-space bound is rescaled towards smaller values by $X_s^{1/4} \leq 1$. A recent publication [76], which we use here, has set the phase-space bound $m_s \gtrsim 190$ eV at the 2σ level for $X_s = 1$. It is worth mentioning that an axion-like particle with mass around the 10^{-22} eV scale (which is not the QCD axion of the av MSM) can also be constrained with phase-space data [77].

Other important bounds on sterile neutrino DM come from the search of X-rays produced by the radiative decay $\tilde{N}_1 \rightarrow \gamma \nu_\alpha$ [78,79]. Since the differential flux produced by the decay of sterile neutrinos depends on the product $X_s \sin^2(2\theta)$, for each chosen value of m_s , the upper limit on $\sin^2(2\theta)$ must weaken by decreasing X_s , rescaling exactly as $1/X_s$ (see also Ref. [80] for a related study). The most recent publications providing this type of X-ray bound used the data collected by the NuSTAR satellite, a space-based X-ray telescope, observing the Milky Way (see [42] for a review) and, more recently, the Andromeda galaxy (M31) [81]. We will take these bounds into account in Section 7.

Now, we describe in turn various production mechanisms for Ω_s as a function of X_s .

4.1. Non-Resonant Production

One important production mechanism of sterile neutrinos is the Dodelson–Widrow (DW) mechanism [38], which we will refer to as the non-resonant production. Precise calculations of Ω_s within this mechanism lead to [82,83]

$$m_s \simeq 3.28 \times \text{keV} \left(\frac{\sin^2(2\theta)}{10^{-8}} \right)^{-0.615} \left(\frac{\Omega_s}{0.26} \right)^{0.5} \left\{ 0.547 \times \text{erfc} \left[-0.969 \left(\frac{T_{\text{QCD}}}{157 \text{ MeV}} \right)^{2.15} \right] \right\}, \tag{22}$$

where erfc is the complementary error function. We have used here a normalization such that the argument of the curly bracket in (22) equals 1 for $T_{\text{QCD}} \simeq 157$ MeV.

In addition to the phase-space and X-ray bounds already discussed, sterile neutrino DM is also subject to structure formation bounds. This is because the typical sterile neutrino momentum distribution exhibits a free-streaming length in the early universe, which modifies the formation of structures. These types of bounds are affected by considerable uncertainties related to, among other things, the simulation of non-linear structure formation as well as the difficulty to observe small-scale structures. Furthermore, this structure formation bound depends on the specific sterile neutrino production mechanism one considers. For the non-resonant production, a study for generic X_s has, however, already been performed in [84]. To have an idea of the orders of magnitude, Ref. [84] found a bound on m_s that is about 10 keV for $X_s = 1$ and 1 keV for $X_s = 0.1$ and so typically stronger than the phase-space bound.

4.2. Resonant Production

The second mechanism to produce sterile neutrino DM is a resonantly enhanced version of the DW mechanism, which relies on a non-vanishing lepton asymmetry L [39,85] and is based on the Mikheyev–Smirnov–Wolfenstein effect [86,87] (see Refs. [88–90] for more recent and precise calculations). In practice, the effective mixing in the plasma is enhanced by L , such that the abundance of active neutrinos allows the creation of sterile neutrinos more efficiently. This asymmetry can be generated dynamically by the heavier sterile neutrinos N_2 and N_3 if their masses are around the GeV scale [91–93]. Moreover, N_2 and N_3 provide a mechanism to generate baryon asymmetry through a different version of leptogenesis [94,95].

The literature to date has focused on the case in which all DM is due to \tilde{N}_1 (i.e., $X_s = 1$), but in our model, the axion also contributes to DM so we need to find more general formulæ that hold for arbitrary X_s . In the non-resonant DW mechanism, the

quantities Ω_s , θ and m_s are related by Equation (22), which has the form $f(\Omega_s, \theta, m_s) = 0$, such that for each fixed value of Ω_s , the DW mechanism is represented by a line in the (θ, m_s) plane. In the resonant production, this function acquires an extra dependence on L , i.e., $f(\Omega_s, \theta, m_s, L) = 0$, and the allowed region in the (θ, m_s) plane is promoted to a band, which is limited by the DW line $f(\Omega_s, \theta, m_s, 0) = 0$. There exists another bound on this band, $f(\Omega_s, \theta, m_s, L_{\max}) = 0$, where L_{\max} is the maximal value of L allowed by observations: the values $L > L_{\max}$ are ruled out because they would excessively change the abundances of light elements produced during Big Bang nucleosynthesis (BBN) [96]. To obtain this bound explicitly for each value of X_s , let us observe that the (dimensionless) yield $Y_s \equiv n_s/s$, where n_s is the sterile neutrino density and s is the entropy density, is related to Ω_s through

$$\Omega_s = \frac{m_s n_s}{\rho_{\text{cr}}} = \frac{m_s Y_s}{\rho_{\text{cr}}/s} \tag{23}$$

so

$$m_s = \frac{X_s \Omega_{\text{DM}} \rho_{\text{cr}}/s}{Y_s}. \tag{24}$$

Note that if we approximate Y_s as a function of θ and L , we only reproduce the linear dependence of Ω_s on m_s found in [39]. Using known results of the literature (see Ref. [42] for a review), one obtains, within this approximation

$$m_s \gtrsim \frac{X_s \Omega_{\text{DM}} \rho_{\text{cr}}/s}{Y_s(\theta, L_{\max})}. \tag{25}$$

This formula tells us that the above-mentioned BBN bound in the resonant production band in the (θ, m_s) plane is rescaled towards smaller values of m_s by $X_s \leq 1$.

5. Sterile Neutrino Dark Matter in a CPT-Symmetric Universe

It was recently pointed out that another mechanism to produce sterile neutrino DM is present if one constructs a CPT-symmetric universe [43,44] in the absence of inflation: the universe before the Big Bang is the CPT reflection of the universe after the Big Bang, so that the time evolution of the universe does not spontaneously violate CPT. In this scenario, a sterile neutrino cosmic abundance is produced according to late-time comoving observers like us just because the vacuum is time dependent. Therefore, unlike the production mechanisms of Section 4, a mixing of the sterile neutrino \tilde{N}_1 responsible for DM and the active neutrinos are not necessary. One can, therefore, set this mixing to zero, requiring the theory to be invariant under a Z_2 symmetry acting on \tilde{N}_1 , which also makes \tilde{N}_1 exactly stable. As a result, the sterile neutrinos produced through this mechanism can easily avoid the X-ray bounds discussed in Section 4.

In our model, inflation can occur and can be triggered by the Higgs, therefore, we do not perform a general study of this possibility⁸. However, it is interesting to see how the calculations of [43,44] change in the presence of another DM component, which in our case is due to the axion.

As shown in [44], assuming that this production mechanism occurs in the radiation-dominated era, the yield of the sterile neutrino can be expressed in terms of its mass m_s :

$$Y_s = \frac{3I}{2\pi^2} \left(\frac{15}{g_*}\right)^{1/4} \left(\frac{m_s}{\hat{\mu}}\right)^{3/2}, \tag{26}$$

where

$$I \equiv \frac{1}{2\pi^2} \int_0^\infty dx x^2 \left[1 - \sqrt{1 - e^{-x^2}}\right] \simeq 0.01276 \tag{27}$$

and $\hat{\mu} \simeq 5.966 \times 10^{18}$ GeV. In this case, the predicted sterile neutrino contribution to the DM energy density is

$$X_s \rho_{\text{DM}} = m_s n_s = m_s Y_s s. \tag{28}$$

Using the known value of ρ_{DM}/s , we find the sterile neutrino mass that is required to account for a fraction X_s of the DM abundance:

$$m_s \simeq 4.8 \times 10^8 \text{ GeV } X_s^{2/5} \left(\frac{g_*}{g_*^{\text{SM}}} \right)^{1/10}, \tag{29}$$

where g_*^{SM} is the effective number of relativistic degrees of freedom in the SM ($g_*^{\text{SM}} \simeq 106.75$ for $T \gg 100 \text{ GeV}$). We note a dependence on X_s and a (milder) dependence on g_* . We also observe that the phase-space lower bound discussed in Section 4 is always satisfied down to negligibly small values of X_s .

Note that in all the sterile neutrino production mechanisms that we have discussed in this section and Section 4, m_s is generically well below (at least six orders of magnitude) the 10^{14} GeV scale. Then, from Equation (4), using the observational bounds on m_i and v , it follows that the impact on the RGEs (see Appendix A) of the Yukawa couplings Y_{ij} is generically negligible compared to the other contributions in Appendix A. This is a good thing because the Y_{ij} contribute negatively to the β -function $\beta_{\lambda_H}^{(1)}$ of the Higgs quartic coupling. Moreover, when \tilde{N}_1 gives a sizeable contribution to DM, the value of f_a required to reproduce the observed DM abundance decreases, as is clear from Section 3, and then so does M_A (cf. Equation (5)). Therefore, the extra scalar starts stabilizing the EW vacuum from smaller energies [1,13,45,46]. It follows that requiring the sterile neutrino to contribute to DM naturally favors EW vacuum stability.

6. Primordial Black Holes as Dark Matter?

PBHs may be generated if the curvature power spectrum $P_{\mathcal{R}}$ has a peak of order $\sim 10^{-2}$ [58], about seven orders of magnitude larger than at ~ 60 e-folds before the end of inflation. An enhancement of $P_{\mathcal{R}}$ generically occurs when the inflaton potential features a (quasi) inflection point⁹ [54–58]. This is the case in CHI [14–16,23,54,55], but in order to see if $P_{\mathcal{R}}$ reaches the required order of magnitude in the ν MSM, a study of this quantity together with other observables is required. We perform this study in this section.

As discussed, e.g., in [23], studying Higgs inflation in the unitary gauge, the potential of the canonically normalized Higgs field ϕ' is given by

$$U_H \equiv \frac{V_H}{\Omega_H^4} = \frac{\lambda_H \phi(\phi')^4}{4(1 + \xi_H \phi(\phi')^2 / \bar{M}_{\text{Pl}}^2)^2}, \tag{30}$$

where $V_H = \lambda_H \phi^4/4$, ϕ is the Higgs field non-minimally coupled to gravity, which is related to ϕ' through

$$\frac{d\phi'}{d\phi} = \Omega_H^{-2} \sqrt{\Omega_H^2 + \frac{3\bar{M}_{\text{Pl}}^2}{2} \left(\frac{d\Omega_H^2}{d\phi} \right)^2}, \tag{31}$$

and Ω_H^2 is defined by

$$\Omega_H^2 \equiv 1 + \frac{2\xi_H |H|^2}{\bar{M}_{\text{Pl}}^2}. \tag{32}$$

In a spatially flat Friedmann–Robertson–Walker geometry, the equations for the spatially homogeneous field $\phi'(t)$ and the cosmological scale factor $a(t)$ are

$$\ddot{\phi}' + \frac{\sqrt{3\dot{\phi}'^2 + 6U_H}}{\sqrt{2}\bar{M}_{\text{Pl}}} \dot{\phi}' + \frac{dU_H}{d\phi'} = 0 \tag{33}$$

and

$$H_1^2 = \frac{\dot{\phi}'^2 + 2U_H}{6\bar{M}_{\text{Pl}}^2}, \tag{34}$$

where a dot represents the derivative with respect to cosmic time t and $H_I \equiv \dot{a}/a$. Inflation in general takes place when¹⁰

$$\epsilon \equiv -\frac{\dot{H}_I}{H_I^2} < 1. \tag{35}$$

Moreover, when

$$\delta \equiv -\frac{\ddot{\phi}'}{H_I \phi'} \tag{36}$$

is small, one can neglect the inertial term in the inflaton in Equation (33) and reduce the problem to a single first order differential equation, leading to the useful slow-roll approximation where the parameters

$$\epsilon_H \equiv \frac{\bar{M}_{\text{Pl}}^2}{2} \left(\frac{1}{U_H} \frac{dU_H}{d\phi'} \right)^2, \quad \eta_H \equiv \frac{\bar{M}_{\text{Pl}}^2}{U_H} \frac{d^2 U_H}{d\phi'^2} \tag{37}$$

are small. These slow-roll functions can be constructed through the more general “horizon flow functions” of Ref. [100].

The number of e-folds is defined by

$$N_e \equiv \int_{t_b}^{t_e} dt H_I(t), \tag{38}$$

where t_e is the time at the end of inflation and t_b is the time when the various inflationary observables such as P_R , the corresponding spectral index n_s and the tensor-to-scalar ratio r are determined through observations. In the slow-roll approximation N_e is expressed as a function of the field ϕ'_b (at t_b) rather than as a function of time,

$$N_e = \int_{\phi'_e}^{\phi'_b} \frac{U_H}{\bar{M}_{\text{Pl}}^2} \left(\frac{dU_H}{d\phi'} \right)^{-1} d\phi', \tag{39}$$

where ϕ'_e is the field value at the end of inflation, and P_R at ϕ'_b can be computed through

$$P_R = \frac{U_H/\epsilon_H}{24\pi^2 \bar{M}_{\text{Pl}}^4}. \tag{40}$$

At the quantum level, these inflationary formulæ remain approximately valid except that one must consider λ_H and ζ_H as functions of ϕ' . In defining these functions, there are well-known ambiguities [5,6,15,101,102]. Here, we adopt the quantization used in [13], which can be embedded in a UV completion of gravity [103–107] (see Refs. [108,109] for reviews). In this approach, the ϕ' -dependence of λ_H and ζ_H is obtained by solving the RGEs given in Appendix A as explained in [13]. The typical shape of the effective inflationary potential (close to criticality) computed in this way is the one shown in¹¹ Figure 2.

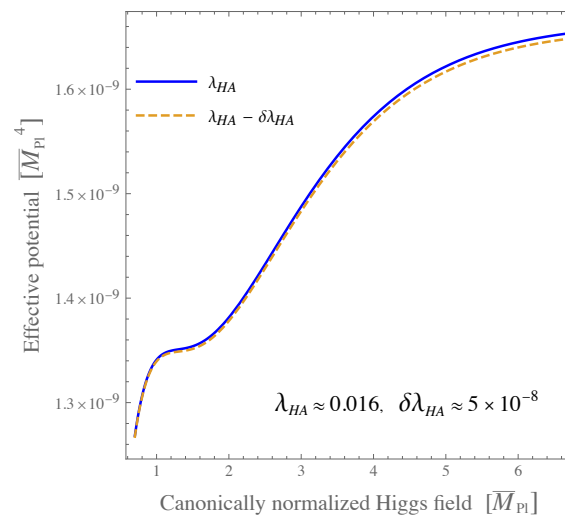


Figure 2. The typical shape of the effective potential as a function of the canonically normalized Higgs field close to criticality (in this plot, we approach the critical regime by varying λ_{HA}).

We find that the above-mentioned requirement to generate PBHs is never satisfied, so PBHs cannot contribute to DM in our model. The reason is the following. Although $P_{\mathcal{R}}$ does have a peak at a time after inflation as a consequence of the inflection point, its height is several orders of magnitude smaller than 10^{-2} when one requires a plausible number of e-folds. This situation is illustrated in Figure 3. In that figure, we approach criticality by varying λ_{HA} , but varying other parameters leads to similar situations. We find that the slow-roll approximation is still reasonably good to give at least the order of magnitude of $P_{\mathcal{R}}$ because both ϵ and δ are well below 1 around the peak of the power spectrum as shown in that figure. Indeed, the numbers of e-folds for λ_{HA} and $\lambda_{HA} - \delta\lambda_{HA}$ are $N_e \simeq 65$ and $N_e \simeq 71$, respectively, while the corresponding values computed with the slow-roll approximation are reasonably close ($N_e \simeq 63$ and $N_e \simeq 70$, respectively). Although the height of the peak of $P_{\mathcal{R}}$ does increase by approaching criticality, it does so at the price of increasing N_e above the bound of [110]: for a pretty low peak of order 10^{-7} , the number of e-folds is already starting to be significantly above ~ 60 . The more we approach criticality, the larger N_e becomes.

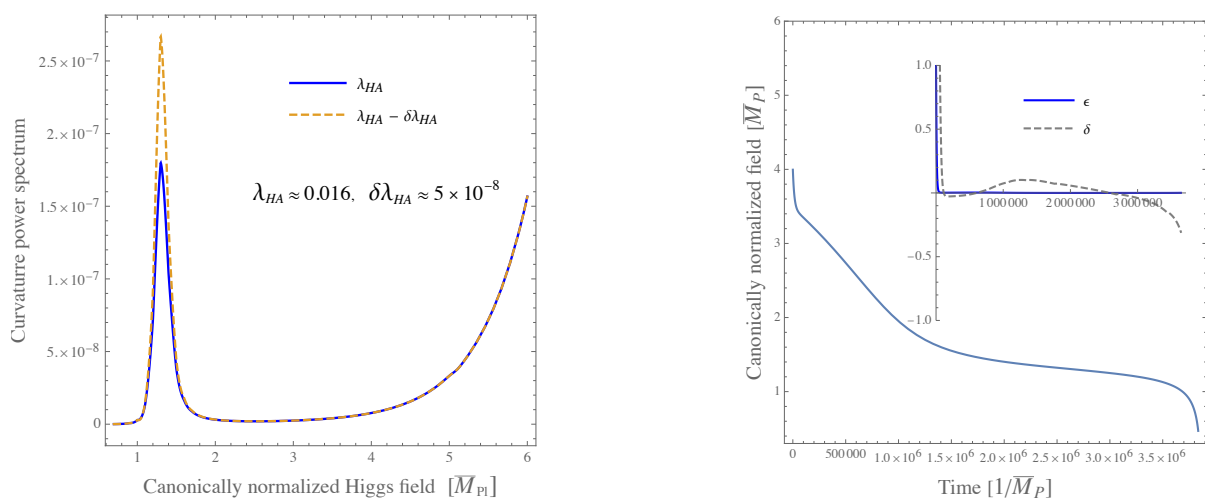


Figure 3. The curvature power spectrum and the canonically normalized (Higgs) field close to criticality (which we approach by varying λ_{HA}). The corresponding values of ϵ and δ are shown as well in an inset of the right plot. The parameters are set as in Figure 2.

In Figure 3, we set the parameters in a way to reproduce the observed neutrino oscillations and have a stable EW vacuum, a viable inflation and baryogenesis through leptogenesis. When all these requirements are satisfied, we always find that PBHs cannot contribute to DM in our model. Essentially, the reason is that the shape of the potential, although apparently able to produce PBH DM, does not have the right quantitative features to do so.

7. Axion–Sterile Neutrino Dark Matter

Having established that the only sources of DM in the ν MSM are axions and sterile neutrinos, we now identify the allowed parameter space in a combined axion–sterile neutrino DM scenario, taking into account all the previously discussed bounds.

Note that in our model, X_s can then be expressed as

$$X_s = 1 - \frac{\Omega_a^{\text{mis}} + \Omega_a^{\text{string}}}{\Omega_{\text{DM}}}, \tag{41}$$

which relates X_s and f_a . We recall that Ω_a^{string} also depends on λ_A (see Equation (8)).

In Figure 4, we show the region corresponding to the resonant sterile neutrino production in the $(\sin^2(2\theta), m_s)$ plane varying X_s . The plot includes the non-resonant production mechanism (the upper line) as a limiting case with vanishing lepton asymmetry (see Sections 4.1 and 4.2). For each value of X_s , we also show the corresponding f_a in two cases. The first case corresponds to a negligible Ω_a^{string} . In the second case, we give the value of the axion decay constant, which we call $f_a^{\text{mis+string}}$, taking into account both Ω_a^{mis} and Ω_a^{string} for $\lambda_A = 0.1$. This is one of the values for which we cannot only account for the whole DM with axions and sterile neutrinos, but we can also reproduce the observed neutrino oscillation phenomenology, baryon asymmetry, have a stable EW vacuum and critical Higgs inflation (in agreement with Planck observations [111,112]) and solve the strong CP problem [13]. Note that moderate variations of λ_A around this value produce very small changes in $f_a^{\text{mis+string}}$ because Ω_a^{string} depends on λ_A only logarithmically.

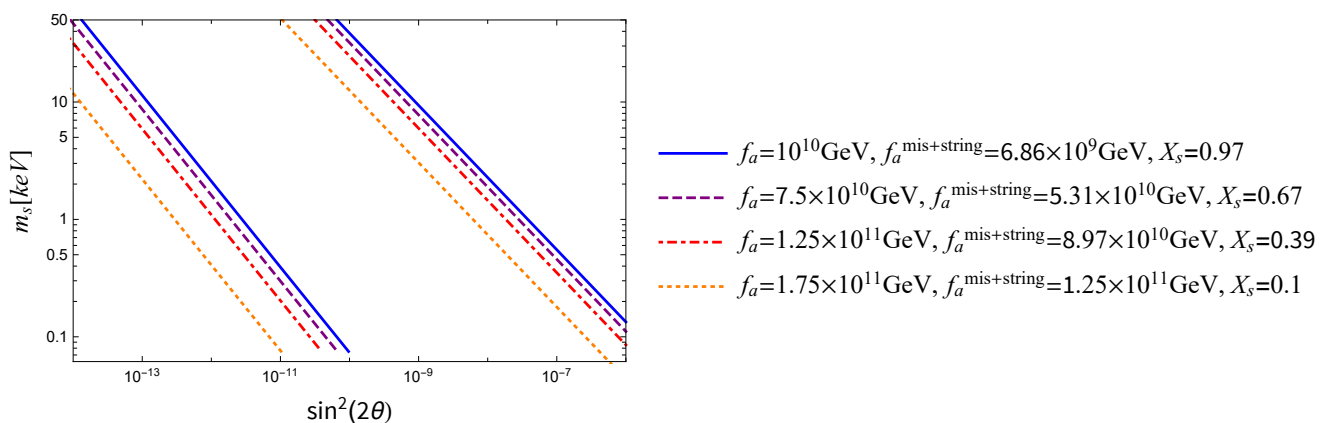


Figure 4. Sterile neutrino production range as the axion decay constant changes. For the first value of the axion decay constant, f_a , we only take into account the misalignment mechanism for axion production. For the second value, $f_a^{\text{mis+string}}$, we take into account both the misalignment mechanism and the decay of topological defects setting $\lambda_A = 0.1$. The upper line corresponds to the non-resonant production and the lower line is the BBN bound discussed in Section 4.2.

In Figure 5, the sterile neutrino production region of Figure 4 is compared with the X-ray and the phase-space bounds discussed in Section 4. In Figure 6, we also add the structure formation bounds discussed in Section 4.1. As shown in Figure 6, an allowed region for non-resonant sterile neutrino production only appears for $X_s \lesssim 0.3$.

Finally, regarding the CPT-symmetric universe discussed in Section 5, note that, interestingly, we can express m_s as a function of f_a with a (mild logarithmic) dependence

on λ_A . This can be obtained by plugging Equation (41) into (29) and using the expressions for Ω_a^{mis} and Ω_a^{string} given in Section 3.

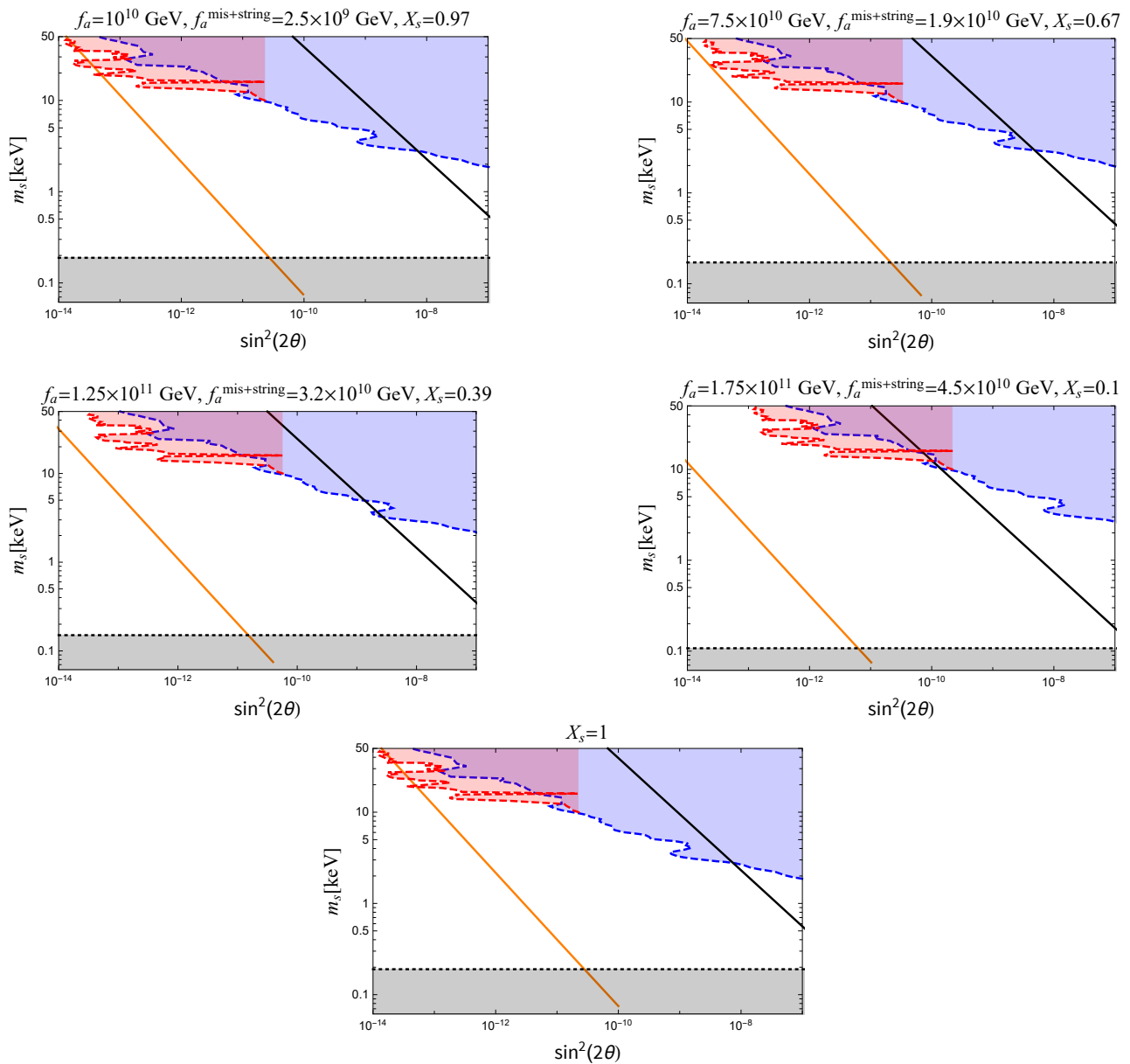


Figure 5. The upper and lower lines of Figure 4 (here depicted in solid black and orange, respectively) compared with the X-ray and phase-space bounds discussed in Section 4 (dashed lines). The X-ray bounds are the upper ones in blue [42] and red [81], while the phase-space ones are the lower ones in black. In this figure, we also provide the corresponding plot for $X_s = 1$ (the bottom one, see Ref. [42] for a review).

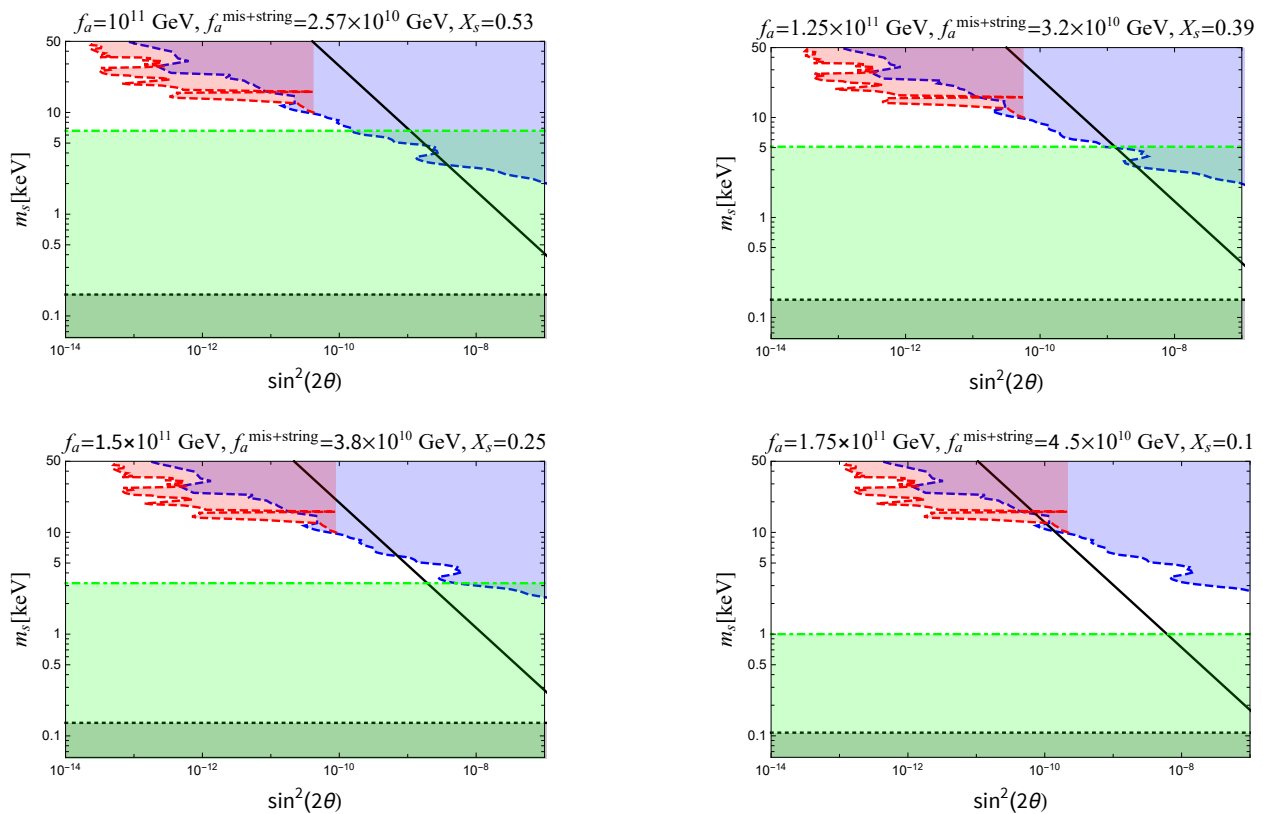


Figure 6. The non-resonant sterile neutrino (black solid lines) and the X-ray and phase-space bounds of Figure 5 together with the structure formation bounds of Section 4.1 (dash-dotted lines).

8. Conclusions

We have analyzed all DM candidates in the av MSM, a simple extension of the SM, originally proposed in [1], which features three sterile neutrinos and the extra fields of the KSVZ QCD axion model. The av MSM is well motivated because it not only accounts for DM, neutrino oscillations and baryon asymmetry, but it also solves the strong CP problem, stabilizes the EW vacuum and can implement CHI (in agreement with the most recent Planck observations).

We have ruled out PBHs as a possible source of DM in this model because $P_{\mathcal{R}}$ has a peak that is several orders of magnitude below the required height. Consequently, DM in this model is generically due to the axion and the lightest sterile neutrino. Imposing several constraints, this result allows us to relate the axion parameters such as f_a and λ_A to the neutrino parameters (m_s and θ).

Requiring the lightest sterile neutrino to contribute to DM in addition to the axion (the only candidate previously considered in the av MSM) has several advantages. We have discussed how this requirement generically enlarges the parameter space with absolute EW stability and, as a result, that is where CHI occurs. This inflationary scenario does not suffer from a too low scale of perturbative unitarity breaking and fine tuning of initial conditions (before inflation). On the other hand, the sterile neutrino DM scenario benefits from the presence of an axion DM component because requiring the lightest sterile neutrino to account only for a fraction $X_s < 1$ of the DM abundance relaxes all the existing constraints on this scenario. Therefore, one can say that axion and sterile neutrino DM mutually reinforce each other in the av MSM.

We plan to keep testing the av MSM with future astrophysical and, in particular, cosmological data, such as those regarding the cosmic microwave background and structure formation.

Author Contributions: Writing—original draft, A.S., S.S.; Writing—review and editing, A.S., S.S. All authors have read and agreed to the published version of the manuscript.

Funding: This research received no external funding.

Institutional Review Board Statement: Not applicable.

Informed Consent Statement: Not applicable.

Data Availability Statement: Data sharing not applicable.

Acknowledgments: We thank G. Ballesteros and A. Urbano for useful discussions and J. Rubio for useful mail communications on primordial black holes in related models.

Conflicts of Interest: The authors declare no conflict of interest.

Appendix A. Renormalization-Group Equations

For a generic coupling g defined in the \overline{MS} renormalization scheme, we write the RGEs as

$$\frac{dg}{d\tau} = \beta_g, \tag{A1}$$

where $d/d\tau \equiv \bar{\mu}^2 d/d\bar{\mu}^2$ and $\bar{\mu}$ is the \overline{MS} renormalization energy scale. The β -functions β_g can also be expanded in loops:

$$\beta_g = \frac{\beta_g^{(1)}}{(4\pi)^2} + \frac{\beta_g^{(2)}}{(4\pi)^4} + \dots, \tag{A2}$$

where $\beta_g^{(n)}/(4\pi)^{2n}$ is the n -loop contribution.

We start from energies much above M_A , M_q and M_{ij} . In this case, the 1-loop RGEs of all relevant couplings are [13]

$$\begin{aligned} \beta_{g_1^2}^{(1)} &= \frac{41g_1^4}{10}, & \beta_{g_2^2}^{(1)} &= -\frac{19g_2^4}{6}, & \beta_{g_3^2}^{(1)} &= -\frac{19g_3^4}{3}, \\ \beta_{y_t^2}^{(1)} &= y_t^2 \left(\frac{9}{2}y_t^2 - 8g_3^2 - \frac{9g_2^2}{4} - \frac{17g_1^2}{20} + \text{Tr}(Y^\dagger Y) \right), \\ \beta_{\lambda_H}^{(1)} &= \left(12\lambda_H + 6y_t^2 - \frac{9g_1^2}{10} - \frac{9g_2^2}{2} + 2\text{Tr}(Y^\dagger Y) \right) \lambda_H \\ &\quad - 3y_t^4 + \frac{9g_2^4}{16} + \frac{27g_1^4}{400} + \frac{9g_2^2g_1^2}{40} + \frac{\lambda_{HA}^2}{2} - \text{Tr}((Y^\dagger Y)^2), \\ \beta_{\lambda_{HA}}^{(1)} &= \left(3y_t^2 - \frac{9g_1^2}{20} - \frac{9g_2^2}{4} + 6\lambda_H \right) \lambda_{HA} \\ &\quad + (4\lambda_A + \text{Tr}(Y^\dagger Y) + 3y^2) \lambda_{HA} + 2\lambda_{HA}^2, \\ \beta_{\lambda_A}^{(1)} &= \lambda_{HA}^2 + 10\lambda_A^2 + 6y^2\lambda_A - 3y^4, \\ \beta_Y^{(1)} &= Y \left[\frac{3}{2}y_t^2 - \frac{9}{40}g_1^2 - \frac{9}{8}g_2^2 + \frac{3}{4}Y^\dagger Y + \frac{1}{2}\text{Tr}(Y^\dagger Y) \right], \\ \beta_{y^2}^{(1)} &= y^2(4y^2 - 8g_3^2), \\ \beta_{\xi_H}^{(1)} &= (1 + 6\xi_H) \left(\frac{y_t^2}{2} + \frac{\text{Tr}(Y^\dagger Y)}{6} - \frac{3g_2^2}{8} - \frac{3g_1^2}{40} + \lambda_H \right) - \frac{\lambda_{HA}}{6}(1 + 6\xi_A), \\ \beta_{\xi_A}^{(1)} &= (1 + 6\xi_A) \left(\frac{y^2}{2} + \frac{2}{3}\lambda_A \right) - \frac{\lambda_{HA}}{3}(1 + 6\xi_H), \end{aligned}$$

where g_3, g_2 and $g_1 = \sqrt{5/3}g_Y$ are the gauge couplings of SM gauge group $SU(3)_c, SU(2)_L$ and $U(1)_Y$, respectively, y_i is the top Yukawa coupling and λ_H is the Higgs quartic coupling appearing in the term $\lambda_H(|H|^2 - v^2)^2$ of the classical potential.

Since the SM couplings evolve in the full range from the EW to the Planck scale, it is appropriate to use for them the 2-loop RGEs¹², which, including the new physics contribution, read:

$$\begin{aligned} \beta_{g_1}^{(2)} &= g_1^4 \left(\frac{199g_1^2}{50} + \frac{27g_2^2}{10} + \frac{44g_3^2}{5} - \frac{17y_t^2}{10} - \frac{3}{10} \text{Tr}(Y^\dagger Y) \right), \\ \beta_{g_2}^{(2)} &= g_2^4 \left(\frac{9g_1^2}{10} + \frac{35g_2^2}{6} + 12g_3^2 - \frac{3y_t^2}{2} - \frac{1}{2} \text{Tr}(Y^\dagger Y) \right), \\ \beta_{g_3}^{(2)} &= g_3^4 \left(\frac{11g_1^2}{10} + \frac{9g_2^2}{2} - \frac{40g_3^2}{3} - 2y_t^2 - y^2 \right), \\ \beta_{y_t}^{(2)} &= +y_t^2 \left[6\lambda_H^2 - \frac{23g_2^4}{4} + y_t^2 \left(-12y_t^2 - 12\lambda_H + 36g_3^2 + \frac{225g_2^2}{16} + \frac{393g_1^2}{80} - \frac{9}{4} \text{Tr}(Y^\dagger Y) \right) \right. \\ &\quad \left. + \frac{1187g_1^4}{600} + 9g_3^2g_2^2 + \frac{19}{15}g_3^2g_1^2 - \frac{9}{20}g_2^2g_1^2 - \frac{932g_3^4}{9} \right. \\ &\quad \left. + \left(\frac{3g_1^2}{8} + \frac{15g_2^2}{8} \right) \text{Tr}(Y^\dagger Y) - \frac{9}{4} \text{Tr}((Y^\dagger Y)^2) + \frac{\lambda_{HA}^2}{2} \right], \\ \beta_{\lambda_H}^{(2)} &= \lambda_H^2 \left[54 \left(g_2^2 + \frac{g_1^2}{5} \right) - 156\lambda_H - 72y_t^2 - 24 \text{Tr}(Y^\dagger Y) \right] \\ &\quad + \lambda_H y_t^2 \left(40g_3^2 + \frac{45g_2^2}{4} + \frac{17g_1^2}{4} - \frac{3}{2}y_t^2 \right) \\ &\quad + \lambda_H \left[\frac{1887g_1^4}{400} - \frac{73g_2^4}{16} + \frac{117g_2^2g_1^2}{40} + \left(\frac{3g_1^2}{4} + \frac{15g_2^2}{4} \right) \text{Tr}(Y^\dagger Y) - \frac{\text{Tr}((Y^\dagger Y)^2)}{2} - 5\lambda_{HA}^2 \right] \\ &\quad + y_t^4 \left(15y_t^2 - 16g_3^2 - \frac{4g_1^2}{5} \right) + y_t^2 \left(\frac{63g_2^2g_1^2}{20} - \frac{9g_2^4}{8} - \frac{171g_1^4}{200} \right) \\ &\quad + \frac{305g_2^6}{32} - \frac{3411g_1^6}{4000} - \frac{289g_2^4g_1^2}{160} - \frac{1677g_2^2g_1^4}{800} \\ &\quad - \left(\frac{9g_1^4}{200} + \frac{3g_1^2g_2^2}{20} + \frac{3g_2^4}{8} \right) \text{Tr}(Y^\dagger Y) + 5 \text{Tr}((Y^\dagger Y)^3) - 3y^2\lambda_{HA}^2 - 2\lambda_{HA}^3. \end{aligned}$$

Here we have corrected a missprint of the RGEs provided in Ref [13]: there are no $g_3^2y^2$ and y^4 contributions to the RGE of λ_H .

The matching at the mass thresholds due to the new scalar A and fermions N_i, q_1 and q_2 is performed as explained in Ref. [13].

Notes

- 1 The strong CP problem is the fine-tuning problem of explaining why the strong interactions do not break CP, while EW ones do. Addressing this fine-tuning problem through a symmetry without doing the same with the Higgs mass and cosmological constant fine-tuning problems appears to be a logical possibility, because the latter problems could be both addressed through anthropic arguments [8–10] (unlike the strong CP one).
- 2 This is the case, e.g., in the ν MSM [47–51], where the axion sector is absent.
- 3 See Refs. [1,13] for a discussion of the remaining observational bounds.
- 4 As usual $h \equiv H_0/(100\text{km s}^{-1}\text{Mpc}^{-1})$, where H_0 is the Hubble constant and ρ_{cr} is the critical energy density.
- 5 In Section 5, we will discuss the recently proposed CPT-symmetric universe of [43,44] where inflation is not required.
- 6 See [73] for a study of this bound when sterile neutrinos account for the whole DM.

- 7 In this case, one neglects the dependence on m_s/T , where T is the photon temperature. This is justified as the resonant production of sterile neutrinos occurs at $T \sim 200$ MeV and $m_s \sim$ keV [93], so $m_s/T \sim 10^{-5}$.
- 8 See Ref. [97] for a recent generalization of the results in [43,44] to non-standard, but also CPT-symmetric early universe cosmologies.
- 9 See also Refs. [98,99] for earlier works on PBH production in inflationary models.
- 10 As usual, the expansion of the universe is nearly exponential for $\epsilon < 1$ and becomes exactly exponential as $\epsilon \rightarrow 0$.
- 11 In that figure, we chose as an example the input values $M_1 = 10^{11}$ GeV, $M_2 = 6.4 \times 10^{13}$ GeV, $M_3 > \bar{M}_{\text{Pl}}$, $f_a \simeq 2.5 \times 10^{10}$ GeV, $\lambda_A(M_A) \simeq 0.1$, $y(M_A) \simeq 0.1$, $\xi_H(M_A) \simeq 14$ and $\xi_A(M_A) \simeq -2.6$.
- 12 In the absence of gravity the RGEs for a generic quantum field theory were computed up to 2-loop order in [113–115].

References

- Salvio, A. A Simple Motivated Completion of the Standard Model below the Planck Scale: Axions and Right-Handed Neutrinos. *Phys. Lett. B* **2015**, *743*, 428. [[CrossRef](#)]
- Kim, J.E. Weak interaction singlet and strong CP invariance. *Phys. Rev. Lett.* **1979**, *43*, 103. [[CrossRef](#)]
- Shifman, M.A.; Vainshtein, A.I.; Zakharov, V.I. Can confinement ensure natural CP invariance of strong interactions? *Nucl. Phys. B* **1980**, *166*, 493. [[CrossRef](#)]
- Bezrukov, F.L.; Shaposhnikov, M. The Standard Model Higgs boson as the inflaton. *Phys. Lett. B* **2008**, *659*, 703. [[CrossRef](#)]
- Bezrukov, F.L.; Magnin, A.; Shaposhnikov, M. Standard Model Higgs boson mass from inflation. *Phys. Lett. B* **2009**, *675*, 88. [[CrossRef](#)]
- Bezrukov, F.; Shaposhnikov, M. Standard Model Higgs boson mass from inflation: Two loop analysis. *J. High Energy Phys.* **2009**, *907*, 89. [[CrossRef](#)]
- Salvio, A. Higgs Inflation at NNLO after the Boson Discovery. *Phys. Lett. B* **2013**, *727*, 234. [[CrossRef](#)]
- Weinberg, S. Anthropic Bound on the Cosmological Constant. *Phys. Rev. Lett.* **1987**, *59*, 2607. [[CrossRef](#)]
- Agrawal, V.; Barr, S.M.; Donoghue, J.F.; Seckel, D. The Anthropic principle and the mass scale of the standard model. *Phys. Rev. D* **1998**, *57*, 5480. [[CrossRef](#)]
- D’Amico, G.; Strumia, A.; Urbano, A.; Xue, W. Direct anthropic bound on the weak scale from supernovae explosions. *Phys. Rev. D* **2019**, *100*, 083013. [[CrossRef](#)]
- Peccei, R.D.; Quinn, H.R. CP Conservation in the Presence of Instantons. *Phys. Rev. Lett.* **1977**, *38*, 1440. [[CrossRef](#)]
- Peccei, R.D.; Quinn, H.R. Constraints Imposed by CP Conservation in the Presence of Instantons. *Phys. Rev. D* **1977**, *16*, 1791. [[CrossRef](#)]
- Salvio, A. Critical Higgs inflation in a Viable Motivated Model. *Phys. Rev. D* **2019**, *99*, 015037. [[CrossRef](#)]
- Hamada, Y.; Kawai, H.; Oda, K.y.; Park, S.C. Higgs Inflation is Still Alive after the Results from BICEP2. *Phys. Rev. Lett.* **2014**, *112*, 241301. [[CrossRef](#)] [[PubMed](#)]
- Bezrukov, F.; Shaposhnikov, M. Higgs inflation at the critical point. *Phys. Lett. B* **2014**, *734*, 249. [[CrossRef](#)]
- Hamada, Y.; Kawai, H.; Oda, K.y.; Park, S.C. Higgs inflation from Standard Model criticality. *Phys. Rev. D* **2015**, *91*, 053008. [[CrossRef](#)]
- Buttazzo, D.; Degrassi, G.; Giardino, P.P.; Giudice, G.F.; Sala, F.; Salvio, A.; Strumia, A. Investigating the near-criticality of the Higgs boson. *J. High Energy Phys.* **2013**, *12*, 1–49. [[CrossRef](#)]
- Burgess, C.P.; Lee, H.M.; Trott, M. Power-counting and the Validity of the Classical Approximation During Inflation. *J. High Energy Phys.* **2009**, *2009*, 103. [[CrossRef](#)]
- Barbon, J.L.F.; Espinosa, J.R. On the Naturalness of Higgs Inflation. *Phys. Rev. D* **2009**, *79*, 081302. [[CrossRef](#)]
- Hertzberg, M.P. On Inflation with Non-minimal Coupling. *J. High Energy Phys.* **2010**, *2010*, 1–14. [[CrossRef](#)]
- Burgess, C.P.; Patil, S.P.; Trott, M. On the Predictiveness of Single-Field Inflationary Models. *J. High Energy Phys.* **2014**, *2014*, 1–31. [[CrossRef](#)]
- Burgess, C.P.; Lee, H.M.; Trott, M. Comment on Higgs Inflation and Naturalness. *J. High Energy Phys.* **2010**, *1007*, 7. [[CrossRef](#)]
- Salvio, A. Initial Conditions for Critical Higgs Inflation. *Phys. Lett. B* **2018**, *780*, 111–117. [[CrossRef](#)]
- Salvio, A.; Mazumdar, A. Classical and Quantum Initial Conditions for Higgs Inflation. *Phys. Lett. B* **2015**, *750*, 194. [[CrossRef](#)]
- Salvio, A. Hearing Higgs with gravitational wave detectors. *J. Cosmol. Astropart. Phys.* **2021**, *6*, 40. [[CrossRef](#)]
- Preskill, J.; Wise, M.; Wilczek, F. Cosmology of the invisible axion. *Phys. Lett. B* **1983**, *120*, 127. [[CrossRef](#)]
- Abbott, L.; Sikivie, P. A cosmological bound on the invisible axion. *Phys. Lett. B* **1983**, *120*, 133. [[CrossRef](#)]
- Dine, M.; Fischler, W. The not so harmless axion. *Phys. Lett. B* **1983**, *120*, 137. [[CrossRef](#)]
- Davis, R.L. Cosmic Axions from Cosmic Strings. *Phys. Lett. B* **1986**, *180*, 225–230. [[CrossRef](#)]
- Harari, D.; Sikivie, P. On the Evolution of Global Strings in the Early Universe. *Phys. Lett. B* **1987**, *195*, 361–365. [[CrossRef](#)]
- Davis, R.L.; Shellard, E.P.S. Do Axions Need Inflation? *Nucl. Phys. B* **1989**, *324*, 167–186. [[CrossRef](#)]
- Battye, R.A.; Shellard, E.P.S. Global string radiation. *Nucl. Phys. B* **1994**, *423*, 260–304. [[CrossRef](#)]
- Nagasawa, M.; Kawasaki, M. Collapse of axionic domain wall and axion emission. *Phys. Rev. D* **1994**, *50*, 4821–4826. [[CrossRef](#)]
- Hiramatsu, T.; Kawasaki, M.; Saikawa, K.; Sekiguchi, T. Production of dark matter axions from collapse of string-wall systems. *Phys. Rev. D* **2012**, *85*, 105020. [[CrossRef](#)]

35. Gorghetto, M.; Hardy, E.; Villadoro, G. Axions from Strings: The Attractive Solution. *J. High Energy Phys.* **2018**, *7*, 151. [[CrossRef](#)]
36. Gorghetto, M.; Hardy, E.; Villadoro, G. More Axions from Strings. *SciPost Phys.* **2021**, *10*, 50. [[CrossRef](#)]
37. Ballesteros, G.; Redondo, J.; Ringwald, A.; Tamarit, C. Standard Model-axion-seesaw-Higgs portal inflation. Five problems of particle physics and cosmology solved in one stroke. *J. Cosmol. Astropart. Phys.* **2017**, *1708*, 1. [[CrossRef](#)]
38. Dodelson, S.; Widrow, L.M. Sterile-neutrinos as dark matter. *Phys. Rev. Lett.* **1994**, *72*, 17–20. [[CrossRef](#)]
39. Shi, X.D.; Fuller, G.M. A New dark matter candidate: Nonthermal sterile neutrinos. *Phys. Rev. Lett.* **1999**, *82*, 2832–2835. [[CrossRef](#)]
40. Kusenko, A. Sterile neutrinos: The Dark side of the light fermions. *Phys. Rep.* **2009**, *481*, 1–28. [[CrossRef](#)]
41. Drewes, M.; Lasserre, T.; Merle, A.; Mertens, S.; Adhikari, R.; Agostini, M.; Ky, N.A.; Araki, T.; Archidiacono, M.; Bahr, M.; et al. A White Paper on keV Sterile Neutrino Dark Matter. *J. Cosmol. Astropart. Phys.* **2017**, *1*, 25.
42. Boyarsky, A.; Drewes, M.; Lasserre, T.; Mertens, S.; Ruchayskiy, O. Sterile neutrino Dark Matter. *Prog. Part. Nucl. Phys.* **2019**, *104*, 1–45. [[CrossRef](#)]
43. Boyle, L.; Finn, K.; Turok, N. CPT-Symmetric Universe. *Phys. Rev. Lett.* **2018**, *121*, 251301. [[CrossRef](#)]
44. Boyle, L.; Finn, K.; Turok, N. The Big Bang, CPT, and neutrino dark matter. *arXiv* **2018**, arXiv:1803.08930.
45. Randjbar-Daemi, S.; Salvio, A.; Shaposhnikov, M. On the decoupling of heavy modes in Kaluza-Klein theories. *Nucl. Phys. B* **2006**, *741*, 236–268. [[CrossRef](#)]
46. Elias-Miro, J.; Espinosa, J.R.; Giudice, G.F.; Lee, H.M.; Strumia, A. Stabilization of the Electroweak Vacuum by a Scalar Threshold Effect. *J. High Energy Phys.* **2012**, *6*, 031. [[CrossRef](#)]
47. Asaka, T.; Blanchet, S.; Shaposhnikov, M. The nuMSM, dark matter and neutrino masses. *Phys. Lett. B* **2005**, *631*, 151–156. [[CrossRef](#)]
48. Asaka, T.; Shaposhnikov, M. The nuMSM, dark matter and baryon asymmetry of the universe. *Phys. Lett. B* **2005**, *620*, 17. [[CrossRef](#)]
49. Asaka, T.; Shaposhnikov, M.; Kusenko, A. Opening a new window for warm dark matter. *Phys. Lett. B* **2006**, *638*, 401–406. [[CrossRef](#)]
50. Asaka, T.; Laine, M.; Shaposhnikov, M. Lightest sterile neutrino abundance within the nuMSM. *J. High Energy Phys.* **2007**, *1*, 91.
51. Canetti, L.; Drewes, M.; Shaposhnikov, M. Sterile Neutrinos as the Origin of Dark and Baryonic Matter. *Phys. Rev. Lett.* **2013**, *110*, 061801. [[CrossRef](#)]
52. Abazajian, K.N.; Kusenko, A. Hidden treasures: Sterile neutrinos as dark matter with miraculous abundance, structure formation for different production mechanisms, and a solution to the σ_8 problem. *Phys. Rev. D* **2019**, *100*, 103513. [[CrossRef](#)]
53. Perez, K.; Ng, K.C.Y.; Beacom, J.F.; Hersh, C.; Horiuchi, S.; Krivonos, R. Almost closing the ν MSM sterile neutrino dark matter window with NuSTAR. *Phys. Rev. D* **2017**, *95*, 123002. [[CrossRef](#)]
54. Garcia-Bellido, J.; Morales, E.R. Primordial black holes from single field models of inflation. *Phys. Dark Univ.* **2017**, *18*, 47–54. [[CrossRef](#)]
55. Ezquiaga, J.M.; Garcia-Bellido, J.; Morales, E.R. Primordial Black Hole production in Critical Higgs Inflation. *Phys. Lett. B* **2018**, *776*, 345–349. [[CrossRef](#)]
56. Ballesteros, G.; Taoso, M. Primordial black hole dark matter from single field inflation. *Phys. Rev. D* **2018**, *97*, 023501. [[CrossRef](#)]
57. Motohashi, H.; Hu, W. Primordial Black Holes and Slow-Roll Violation. *Phys. Rev. D* **2017**, *96*, 063503. [[CrossRef](#)]
58. Hertzberg, M.P.; Yamada, M. Primordial Black Holes from Polynomial Potentials in Single Field Inflation. *Phys. Rev. D* **2018**, *97*, 083509. [[CrossRef](#)]
59. Carr, B.; Kohri, K.; Sendouda, Y.; Yokoyama, J. Constraints on Primordial Black Holes. *arXiv* **2020**, arXiv:2002.12778.
60. Luzio, L.D.; Giannotti, M.; Nardi, E.; Visinelli, L. The landscape of QCD axion models. *Phys. Rep.* **2020**, *870*, 1–117. [[CrossRef](#)]
61. Esteban, I.; Gonzalez-Garcia, M.C.; Maltoni, M.; Schwetz, T.; Zhou, A. The fate of hints: Updated global analysis of three-flavor neutrino oscillations. *J. High Energy Phys.* **2020**, *9*, 178. [[CrossRef](#)]
62. de Salas, P.F.; Forero, D.V.; Gariazzo, S.; Martínez-Miravé, P.; Mena, O.; Ternes, C.A.; Tórtola, M.; Valle, J.W.F. 2020 Global reassessment of the neutrino oscillation picture. *arXiv* **2020**, arXiv:2006.11237.
63. Zyla, P.A.; et al. Particle Data Group. *Prog. Theor. Exp. Phys.* **2020**, 083C01. Available online: <https://pdg.lbl.gov/2020/tables/rpp2020-sum-quarks.pdf> (accessed on 22 September 2021).
64. Hagiwara, K.; Hikasa, K.; Nakamura, K.; Tanabashi, M.; Aguilar-Benitez, M.; AMSler, C.; Barnett, R.M.; Burchat, P.R.; Carone, C.D.; Lugovsky, V.S.; et al. Particle Data Group. *Phys. Rev. D* **2018**, *98*, 030001. Available online: <http://pdg.lbl.gov/2018/tables/rpp2018-sum-gauge-higgs-bosons.pdf> (accessed on 22 September 2021).
65. Bethke, S. World Summary of α_s (2012). *Nucl. Phys. Proc. Suppl.* **2013**, *234*, 229. [[CrossRef](#)]
66. Petreczky, P.; Schadler, H.P.; Sharma, S. The topological susceptibility in finite temperature QCD and axion cosmology. *Phys. Lett. B* **2016**, *762*, 498–505. [[CrossRef](#)]
67. Borsanyi, S.; Fodor, Z.; Guenther, J.; Kampert, K.H.; Katz, S.D.; Kawanai, T.; Kovacs, T.G.; Mages, S.W.; Pasztor, A.; Pittler, F.; et al. Calculation of the axion mass based on high-temperature lattice quantum chromodynamics. *Nature* **2016**, *539*, 69–71. [[CrossRef](#)] [[PubMed](#)]
68. Alion, T.; Back, J.J.; Bashyal, A.; Bass, M.; Bishai, M.; Cherdack, D.; Diwan, M.; Djurcic, Z.; Evans, J.; Fernandez-Martinez, E.; et al. Particle Data Group. Review of Particle Physics. *Phys. Rev. D* **2016**. Available online: <https://arxiv.org/pdf/1606.09550.pdf> (accessed on 22 September 2021).

69. Bezrukov, F.; Gorbunov, D.; Shaposhnikov, M. On initial conditions for the Hot Big Bang. *J. Cosmol. Astropart. Phys.* **2009**, *906*, 29. [[CrossRef](#)]
70. Garcia-Bellido, J.; Figueroa, D.G.; Rubio, J. Preheating in the Standard Model with the Higgs-Inflaton coupled to gravity. *Phys. Rev. D* **2009**, *79*, 063531. [[CrossRef](#)]
71. Kawasaki, M.; Saikawa, K.; Sekiguchi, T. Axion dark matter from topological defects. *Phys. Rev. D* **2015**, *91*, 065014. [[CrossRef](#)]
72. Tremaine, S.; Gunn, J.E. Dynamical Role of Light Neutral Leptons in Cosmology. *Phys. Rev. Lett.* **1979**, *42*, 407–410. [[CrossRef](#)]
73. Gorbunov, D.; Khmel'nitsky, A.; Rubakov, V. Constraining sterile neutrino dark matter by phase-space density observations. *J. Cosmol. Astropart. Phys.* **2008**, *10*, 41. [[CrossRef](#)]
74. Boyanovsky, D.; de Vega, H.J.; Sanchez, N. Constraints on dark matter particles from theory, galaxy observations and N-body simulations. *Phys. Rev. D* **2008**, *77*, 043518. [[CrossRef](#)]
75. de Vega, H.J.; Sanchez, N.G. Model independent analysis of dark matter points to a particle mass at the keV scale. *Mon. Not. R. Astron. Soc.* **2010**, *404*, 885. [[CrossRef](#)]
76. Savchenko, D.; Rudakovskiy, A. New mass bound on fermionic dark matter from a combined analysis of classical dSphs. *Mon. Not. R. Astron. Soc.* **2019**, *487*, 5711–5720. [[CrossRef](#)]
77. de Vega, H.J.; Sanchez, N.G. Galaxy phase-space density data exclude Bose-Einstein condensate Axion Dark Matter. *arXiv* **2014**, arXiv:1401.1214.
78. Pal, P.B.; Wolfenstein, L. Radiative Decays of Massive Neutrinos. *Phys. Rev. D* **1982**, *25*, 766. [[CrossRef](#)]
79. Barger, V.D.; Phillips, R.J.N.; Sarkar, S. Remarks on the KARMEN anomaly. *Phys. Lett. B* **1995**, *352*, 365–371. [[CrossRef](#)]
80. Benso, C.; Brdar, V.; Lindner, M.; Rodejohann, W. Prospects for Finding Sterile Neutrino Dark Matter at KATRIN. *Phys. Rev. D* **2019**, *100*, 115035. [[CrossRef](#)]
81. Ng, K.C.Y.; Roach, B.M.; Perez, K.; Beacom, J.F.; Horiuchi, S.; Krivonos, R.; Wik, D.R. New Constraints on Sterile Neutrino Dark Matter from *NuSTAR* M31 Observations. *Phys. Rev. D* **2019**, *99*, 083005. [[CrossRef](#)]
82. Abazajian, K. Production and evolution of perturbations of sterile neutrino dark matter. *Phys. Rev. D* **2006**, *73*, 063506. [[CrossRef](#)]
83. Abazajian, K.N. Sterile neutrinos in cosmology. *Phys. Rep.* **2017**, *711–712*, 1–28. [[CrossRef](#)]
84. Palazzo, A.; Cumberbatch, D.; Slosar, A.; Silk, J. Sterile neutrinos as subdominant warm dark matter. *Phys. Rev. D* **2007**, *76*, 103511. [[CrossRef](#)]
85. Abazajian, K.; Fuller, G.M.; Patel, M. Sterile neutrino hot, warm, and cold dark matter. *Phys. Rev. D* **2001**, *64*, 023501. [[CrossRef](#)]
86. Wolfenstein, L. Neutrino Oscillations in Matter. *Phys. Rev. D* **1978**, *17*, 2369–2374. [[CrossRef](#)]
87. Mikheyev, S.P.; Smirnov, A.Y. Resonance Amplification of Oscillations in Matter and Spectroscopy of Solar Neutrinos. *Sov. J. Nucl. Phys.* **1985**, *42*, 913–917.
88. Ghiglieri, J.; Laine, M. Improved determination of sterile neutrino dark matter spectrum. *J. High Energy Phys.* **2015**, *11*, 171. [[CrossRef](#)]
89. Venumadhav, T.; Cyr-Racine, F.Y.; Abazajian, K.N.; Hirata, C.M. Sterile neutrino dark matter: Weak interactions in the strong coupling epoch. *Phys. Rev. D* **2016**, *94*, 043515. [[CrossRef](#)]
90. Bodeker, D.; Klaus, A. Sterile neutrino dark matter: Impact of active-neutrino opacities. *J. High Energy Phys.* **2020**, *7*, 218. [[CrossRef](#)]
91. Laine, M.; Shaposhnikov, M. Sterile neutrino dark matter as a consequence of nuMSM-induced lepton asymmetry. *J. Cosmol. Astropart. Phys.* **2008**, *6*, 31. [[CrossRef](#)]
92. Canetti, L.; Drewes, M.; Frossard, T.; Shaposhnikov, M. Dark Matter, Baryogenesis and Neutrino Oscillations from Right Handed Neutrinos. *Phys. Rev. D* **2013**, *87*, 093006. [[CrossRef](#)]
93. Eijima, S.; Shaposhnikov, M.; Timiryasov, I. Freeze-in generation of lepton asymmetries after baryogenesis in the ν MSM. *arXiv* **2020**, arXiv:2011.12637.
94. Akhmedov, E.K.; Rubakov, V.A.; Smirnov, A.Y. Baryogenesis via neutrino oscillations. *Phys. Rev. Lett.* **1998**, *81*, 1359. [[CrossRef](#)]
95. Drewes, M.; Garbrecht, B. Leptogenesis from a GeV Seesaw without Mass Degeneracy. *J. High Energy Phys.* **2013**, *3*, 96. [[CrossRef](#)]
96. Serpico, P.D.; Raffelt, G.G. Lepton asymmetry and primordial nucleosynthesis in the era of precision cosmology. *Phys. Rev. D* **2005**, *71*, 127301. [[CrossRef](#)]
97. Duran, A.; Morrison, L.; Profumo, S. Sterile Neutrino Dark Matter from Generalized CPT-Symmetric Early-Universe Cosmologies. *arXiv* **2021**, arXiv:2103.08626.
98. Kohri, K.; Lyth, D.H.; Melchiorri, A. Black hole formation and slow-roll inflation. *J. Cosmol. Astropart. Phys.* **2008**, *4*, 38. [[CrossRef](#)]
99. Kohri, K.; Lin, C.M.; Matsuda, T. Primordial black holes from the inflating curvaton. *Phys. Rev. D* **2013**, *87*, 103527. [[CrossRef](#)]
100. Schwarz, D.J.; Terrero-Escalante, C.A.; Garcia, A.A. Higher order corrections to primordial spectra from cosmological inflation. *Phys. Lett. B* **2001**, *517*, 243–249. [[CrossRef](#)]
101. Bezrukov, F.; Rubio, J.; Shaposhnikov, M. Living beyond the edge: Higgs inflation and vacuum metastability. *Phys. Rev. D* **2015**, *92*, 083512. [[CrossRef](#)]
102. Bezrukov, F.; Pauly, M.; Rubio, J. On the robustness of the primordial power spectrum in renormalized Higgs inflation. *J. Cosmol. Astropart. Phys.* **2018**, *1802*, 40. [[CrossRef](#)]
103. Salvio, A.; Strumia, A. Agravity. *J. High Energy Phys.* **2014**, *1406*, 80. [[CrossRef](#)]
104. Salvio, A. Solving the Standard Model Problems in Softened Gravity. *Phys. Rev. D* **2016**, *94*, 096007. [[CrossRef](#)]
105. Salvio, A.; Strumia, A. Agravity up to infinite energy. *Eur. Phys. J. C* **2018**, *78*, 124. [[CrossRef](#)] [[PubMed](#)]

106. Salvio, A. Metastability in Quadratic Gravity. *Phys. Rev. D* **2019**, *99*, 103507. [[CrossRef](#)]
107. Salvio, A. Quasi-Conformal Models and the Early Universe. *Eur. Phys. J. C* **2019**, *79*, 750. [[CrossRef](#)]
108. Salvio, A. Quadratic Gravity. *Front. Phys.* **2018**, *6*, 77. [[CrossRef](#)]
109. Salvio, A. Dimensional Transmutation in Gravity and Cosmology. *Int. J. Mod. Phys. A* **2021**, *36*, 2130006. [[CrossRef](#)]
110. Liddle, A.R.; Leach, S.M. How long before the end of inflation were observable perturbations produced? *Phys. Rev. D* **2003**, *68*, 103503. [[CrossRef](#)]
111. Ade, P.A.R.; Aghanim, N.; Arnaud, M.; Arroja, F.; Ashdown, M.; Aumont, J.; Baccigalupi, C.; Ballardini, M.; Banday, A.J.; Barreiro, R.B.; et al. Planck 2015 results. XX. Constraints on inflation. *Astron. Astrophys.* **2016**, *594*, A20.
112. Akrami, Y.; Arroja, F.; Ashdown, M.; Aumont, J.; Baccigalupi, C.; Ballardini, M.; Banday, A.J.; Barreiro, R.B.; Bartolo, N.; Basak, S.; et al. Planck 2018 results. X. Constraints on inflation. *Astron. Astrophys.* **2020**, *641*, A10.
113. Machacek, M.E.; Vaughn, M.T. Two Loop Renormalization Group Equations in a General Quantum Field Theory. 1. Wave Function Renormalization. *Nucl. Phys.* **1983**, *B222*, 83. [[CrossRef](#)]
114. Machacek, M.E.; Vaughn, M.T. Two Loop Renormalization Group Equations in a General Quantum Field Theory. 2. Yukawa Couplings. *Nucl. Phys.* **1984**, *B236*, 221. [[CrossRef](#)]
115. Machacek, M.E.; Vaughn, M.T. Two Loop Renormalization Group Equations in a General Quantum Field Theory. 3. Scalar Quartic Couplings. *Nucl. Phys.* **1985**, *B249*, 70. [[CrossRef](#)]